

Robust design optimization of the vibrating rotor shaft system subjected to selected dynamic constraints

R. Stocki*, T. Szolc, P. Tazowski, J. Knabel

*Institute of Fundamental Technological Research, Polish Academy of Sciences
ul. Pawińskiego 5B, 02-106 Warsaw, Poland*

Abstract

The commonly observed nowadays tendency to weight minimization of rotor-shafts of the rotating machinery leads to a decrease of shaft bending rigidity making a risk of dangerous stress concentrations and rubbing effects more probable. Thus, a determination of the optimal balance between reducing the rotor-shaft weight and assuring its admissible bending flexibility is a major goal of this study. The random nature of residual unbalances of the rotor-shaft as well as randomness of journal bearing stiffness have been taken into account in the framework of robust design optimization. Such a formulation of the optimization problem leads to the optimal design that combines an acceptable structural weight with the robustness with respect to uncertainties of residual unbalances – the main source of bending vibrations causing the rubbing effects. The applied robust optimization technique is based on using Latin hypercubes in scatter analysis of the vibration response. The so-called optimal Latin hypercubes are used as experimental plans for building kriging approximations of the objective and constraint functions. The proposed method has been applied for the optimization of the typical single-span rotor-shaft of the 8-stage centrifugal compressor.

Keywords: rotor-shaft system, robust design optimization, lateral vibrations, rubbing effects, random unbalance distribution

1. Introduction

Excessive stress concentrations and rubbing effects occurring between stators and rotors attached to flexible shafts affected by unavoidable lateral vibrations are

*Corresponding author: rstocki@ippt.gov.pl

very detrimental phenomena from the viewpoint of effective and safe exploitation of the rotating machines. The modern, responsible and heavily affected rotating machines must assure possibly high level of reliability, durability and safety in operation. This is why, their designs have to be performed very thoroughly in order to obtain relatively small magnitude of unavoidable dynamic excitation, e.g. due to residual unbalance, gas-pressure forces or electromagnetic forces, as well as optimal geometric, structural and material parameters resulting in minimal material stress during operation. According to the above, several methods for rotor-machine optimum design have been developed and applied so far by many authors in order to satisfy all these difficult technological criteria. Optimization techniques allow determining detailed geometrical dimensions and material layer structure of the rotor-shaft. For example, in [1] the geometrical structure of the welded drum-type low-pressure rotors of steam turbogenerators was optimized and in [2] the optimal thickness values of the steel and ceramic layers of the shaft cross-section have been determined by the use of the finite element method and the boundary element method. The rotor-shaft optimal parameters together with the most convenient bearing support properties and system unbalance distributions resulting in minimal bending vibrations were calculated in [3–6]. In [3, 4] the iterative procedure for the optimum design of the rotor-bearing system was applied in order to set the fundamental vibration modes possibly weakly sensitive to synchronous excitations at nominal operational speeds. Similar task has been solved in [5] by the use of various optimization approaches, where the Gauss-Newton method appeared as the most convenient one. In [6] a minimization of the rotor-shaft bending vibrations was performed by means of the balancing optimization technique based on the linear matrix inequality method.

All the rotor-shaft optimization problems mentioned above were considered as deterministic. The values of model parameters were assumed to be precisely known, not exhibiting any stochastic scatter. Moreover, majority of the applied optimization procedures adjust the rotor-shaft system for possibly effective and safe operation in steady-state, nominal, out of resonance working conditions.

While aiming at realistic modeling of rotor-shaft systems, neither the deterministic parameter assumption nor the restriction to the steady-state operating conditions seem to be necessary or justified in formulating the optimization problem. The main objective of the presented study is to account for inherently random nature of residual unbalances as well as stiffness parameters of journal bearings by formulating the rotor-shaft optimization problem in the framework of the robust design optimization, see e.g. [7–9] for a comprehensive robust design optimization survey.

The other goal is to find the optimal design that is robust with respect to parameter uncertainties even when the rotor-shaft of a rotating machine is subjected to considerable bending or torsional resonance vibrations. Contrary to e.g. typical power-plant steam turbogenerators or off-shore gas expanders, many rotor machines, such as compressors, pumps, blowers or fans driven by electric motors, do not operate continuously in nominal working conditions, properly located possibly far away from vibration resonance zones, but they are being frequently switched-on and -off, which leads to their systematic start-ups and run-downs. Taking into account the commonly observed now tendency of designing relatively light-weight, so called overcritical, rotor-shafts of rotating machines, each passage from the stand-still into the nominal working conditions during start-up and from the nominal working conditions back - to the stand still during run-down is associated with passages through more or less severe resonances of lateral and torsional vibrations, where these of the fundamental, i.e. the lowest, natural frequencies are the most dangerous for the rotor-shaft material fatigue. Because of these reasons, for a such group of rotating machines the rotor-shaft optimization should be performed not for the nominal working conditions only, but for the operation during the most severe bending or torsional vibration resonances.

In the presented paper the object of consideration is the typical single-span rotor-shaft of the 8-stage centrifugal compressor driven by the electric motor. Since the rotor-machine shafts are usually connected with driving motors by means of flexurally and torsionally flexible couplings, the machine rotor-shafts and the electric motor rotors are dynamically isolated from each other and thus their lateral and torsional vibrations can be very often regarded as mutually uncoupled. According to the above, optimization procedures based on the thorough dynamic analyses for the considered rotating machine drive system can be focused on the compressor rotor-shaft only.

2. Description of the hybrid mechanical model

In order to obtain sufficiently reliable results of numerical simulations, together with a reasonable computational efficiency, the vibrating rotor-shaft system of a rotor machine is usually modeled by means of the one-dimensional finite elements of the beam-type. Nevertheless, such models are characterized by relatively high number of degrees of freedom in the range between hundreds and even thousands. Moreover, e.g. for the Monte Carlo simulation performed for numerous sets of design parameters and external excitations, the discretization mesh density of the finite element model must be appropriately modified in each case. Thus, for

such large finite-element models, proper algorithms reducing number of degrees of freedom have to be employed in order to shorten computer simulation times. It is to remember that such reductions of degrees of freedom are troublesome and can lead to computational inaccuracies. According to the above, similarly as in [10, 11], in order to avoid the abovementioned drawbacks of the finite element approach and to maintain the obvious advantages of this method, in this paper the dynamic analysis of the entire rotating system are performed by means of the one-dimensional hybrid structural model consisting of continuous visco-elastic macro-elements and discrete oscillators. This model is employed here for eigenvalue analyses as well as for the random numerical simulations of lateral vibrations of the rotor-shaft. In the model successive cylindrical segments of the stepped rotor-shaft are substituted by flexurally and torsionally deformable cylindrical macro-elements of continuously distributed inertial-visco-elastic properties. A typical i -th continuous visco-elastic macro-element is presented in Fig. 1.

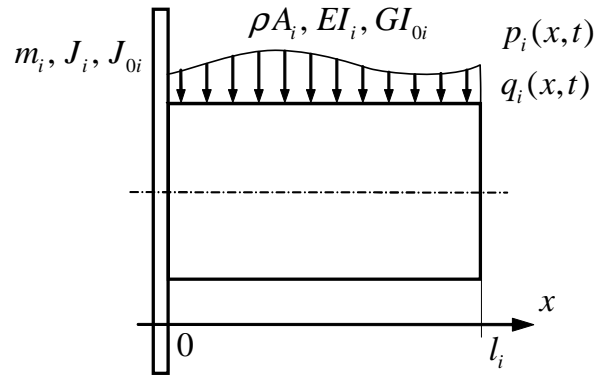


Figure 1: Flexurally and torsionally deformable continuous visco-elastic macro-element.

In this figure symbols A_i , I_i and I_{0i} denote respectively the cross-sectional area, the diametric and polar geometric moment of inertia, $i = 1, 2, \dots, n$, where n is the total number of macro-elements in the considered hybrid model. The transverse and torsional external loads continuously distributed along the macro-element length l_i , if any, are described by the two-argument functions $p_i(x, t)$ and $q_i(x, t)$, where x is the spatial coordinate and t denotes time. With an accuracy that is sufficient for practical purposes, in the proposed hybrid model of the rotor-shaft system, some heavy rotors or coupling disks can be represented by rigid bodies attached to the macro-element extreme cross sections, as shown in Fig. 1. Here, symbols m_i , J_i and J_{0i} denote respectively the mass, the diametric and polar

mass moment of inertia of this rigid body. Each journal bearing is represented by the use of a dynamic oscillator of two degrees of freedom, where apart from the oil-film interaction also the visco-elastic properties of the bearing housing and foundation are taken into consideration. This bearing model makes possible to represent with relatively high accuracy kinetostatic and dynamic anisotropic and anti-symmetric properties of the oil-film in the form of constant or variable stiffness and damping coefficients. An example of such a hybrid model of the mentioned above centrifugal compressor rotor-shaft is presented in Fig. 2. This compressor rotor-shaft is supported on two journal bearings, where the additional support in its mid-span caused by the aero-dynamic cross-coupling effect is taken into consideration.

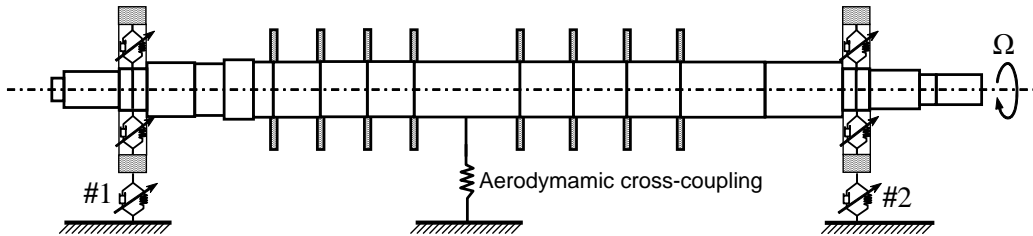


Figure 2: Hybrid mechanical model of the compressor rotor-shaft.

For relatively small magnitude of the rotor-shaft system unbalance, e.g. due to residual static and dynamic unbalance of the shaft segments and rotor-disks, the coupling effect between the torsional and bending vibrations is usually negligible, which has been demonstrated in [10] and in other publications written by numerous authors. Moreover, since in majority of fluid-flow rotating machinery operating in steady-state conditions the fluctuating components of dynamic torques transmitted by their rotor-shaft systems are very small, in the carried out considerations only flexural excitation causing bending vibrations due to unbalances is going to be taken into account. Thus, simulations of torsional forced vibrations will not be performed.

In the hybrid model, flexural motion of cross sections of each visco-elastic macro-element of the length l_i is governed by the partial differential equations derived using the Timoshenko and Rayleigh rotating beam theory. The motion equation for the visco-elastically supported rotating Rayleigh beam with a circular

cross-section has the following form

$$\begin{aligned}
& EI_i \left(1 + e \left(\frac{\partial}{\partial t} - j\Omega(t) \right) \right) \frac{\partial^4 v_i(x, t)}{\partial x^4} - \rho I_i \frac{\partial^4 v_i(x, t)}{\partial x^2 \partial t^2} + \\
& j\Omega(t) I_{0i} \frac{\partial^3 v_i(x, t)}{\partial x^2 \partial t} + \rho A_i \frac{\partial^2 v_i(x, t)}{\partial t^2} = p_i(x, t)
\end{aligned} \tag{1}$$

where $v_i(x, t) = u_i(x, t) + jw_i(x, t)$, $u_i(x, t)$ being the lateral displacement in the vertical direction and $w_i(x, t)$ the lateral displacement in the horizontal direction, j denotes the imaginary number, $\Omega(t)$ is the current average, i.e. corresponding to rigid body motion, shaft rotational speed, e denotes the retardation time for beam flexural deformation, ρ denotes the material density, $i = 1, 2, \dots, n$, and n is the total number of macro-elements in the hybrid model. It is to remark that in the case of the rotating shaft with a circular cross-section the gyroscopic forces mutually couple in (1) bending vibrations in two perpendicular planes, e.g. in the vertical and the horizontal one. The same coupling effect is caused by the rotational speed dependent material damping term.

Similarly as in [10, 11], mutual connections of the successive macro-elements creating the stepped shaft as well as their interactions with the supports and rigid bodies representing the heavy rotors are described by equations of boundary conditions. These equations contain geometrical conditions of conformity for translational and rotational displacements of extreme cross sections of the adjacent $(i - 1)$ -th and the i -th elastic macro-elements. The second group of boundary conditions formulated for these macro-elements are dynamic ones, which in general contain linear, nonlinear and parametric equations of equilibrium for external forces, static and dynamic unbalance forces and moments, inertial, elastic and external damping forces, support reactions and gyroscopic moments. By means of the dynamic boundary conditions there are also described shaft interactions with discrete oscillators representing shaft supports in journal bearings. Here, similarly as in [11], such boundary conditions contain anti-symmetrical terms with cross-coupling oil-film stiffness components, which couple shaft bending vibrations in two mutually perpendicular planes. In these equations the stiffness and damping coefficients can be constant or variable, when non-linear properties of the oil-film are taken into consideration.

The solution for the forced bending vibration analysis has been obtained using the analytical - computational approach demonstrated in detail in [10, 11]. Solving the differential eigenvalue problem for the linearized orthogonal system and an application of the Fourier solutions in the form of series in orthogonal eigen-

functions leads to the set of modal equations in the Lagrange coordinates

$$\mathbf{M}_0 \ddot{\mathbf{r}}(t) + \mathbf{D}(\Omega(t)) \dot{\mathbf{r}}(t) + \mathbf{K}(\Omega(t)) \mathbf{r}(t) = \mathbf{F}(\Omega^2(t), \Theta(t)), \quad (2)$$

where:

$$\begin{aligned} \mathbf{D}(\Omega(t)) &= \mathbf{D}_0 + \mathbf{D}_g(\Omega(t)), \\ \mathbf{K}(\Omega(t)) &= \mathbf{K}_0 + \mathbf{K}_b + \mathbf{K}_d(\Omega(t)), \quad \Theta(t) = \int_0^t \Omega(\tau) d\tau \end{aligned}$$

The symbols \mathbf{M}_0 , \mathbf{K}_0 denote, respectively, the constant diagonal modal mass and stiffness matrices, \mathbf{D}_0 is the constant symmetrical damping matrix and $\mathbf{D}_g(\Omega(t))$ denotes the skew-symmetrical matrix of gyroscopic effects. Anti-symmetric elastic properties of the journal bearings are described by the skew-symmetrical matrix \mathbf{K}_b . Anti-symmetric effects due to Kelvin-Voigt material damping model of the rotating shaft are expressed by the skew-symmetrical matrix $\mathbf{K}_d(\Omega(t))$ and the symbol $\mathbf{F}(\Omega^2(t), \Theta(t))$ denotes the external excitation vector due to the unbalance and gravitational forces. The Lagrange coordinate vector $\mathbf{r}(t)$ consists of the unknown time functions $\zeta_m(t)$ in the Fourier solutions, $m = 1, 2, \dots$. The number of equations (2) corresponds to the number of bending eigenmodes taken into consideration in the range of frequency of interest. These equations are mutually coupled by the out-of-diagonal terms in matrices \mathbf{D} and \mathbf{K} . The out-of-diagonal terms are results of regarding the gyroscopic effects as well as skew-symmetrical bearing and internal damping characteristics as response dependent external excitations expanded in series in the base of orthogonal analytical eigenfunctions. A fast convergence of the applied Fourier solution enables us to reduce the appropriate number of the modal equations to solve in order to obtain a sufficient accuracy of results in the given range of frequency. Here, it is necessary to solve only $10 \div 20$ coupled modal equations (2), even in cases of complex mechanical systems, contrary to the classical one-dimensional beam finite element formulation usually leading to large numbers of motion equations corresponding each to more than one hundred or many hundreds degrees of freedom (if the artificial and often error-prone model reduction algorithms are not applied). However, due to the natural, continuous distribution of inertial-visco-elastic properties of the beam macro-elements the hybrid modeling assures at least the same or even better representation of real objects as well as its mathematical description is formally strict and demonstrates clearly the qualitative system properties. Thus, the proposed approach is much more convenient for a stable and efficient numerical simulation.

In a general case, i.e. for the variable in time shaft average rotational speed $\Omega(t)$ during system start-ups or run-downs, in order to obtain the system's dynamic response equations (2) can be solved by means of a direct integration. However, for the constant shaft rotational speed Ω and for constant stiffness and damping coefficients of the bearing supports equations (2) become a system of linear ordinary differential equations with constant coefficients and harmonic external excitation due to the residual unbalances. Such excitation can be expressed as

$$\mathbf{F}(\Omega^2, \Omega t) = \mathbf{Q} + \mathbf{P}(\Omega^2) \cos(\Omega t) + \mathbf{R}(\Omega^2) \sin(\Omega t) \quad (3)$$

where vectors $\mathbf{P}(\Omega^2)$, $\mathbf{R}(\Omega^2)$ contain the modal components of unbalance amplitudes and vector \mathbf{Q} contains the modal components of the rotor-shaft static gravitational load. Then, in order to obtain the system's steady-state dynamic response, an analytical solution of equations (2) is very convenient. For the mentioned above harmonic excitation (3) the induced steady-state vibrations are also harmonic with the same synchronous circular frequency Ω . Thus, the analytical solutions for the successive modal functions $\xi_m(t)$ contained in vector $\mathbf{r}(t)$ can be assumed in the following form:

$$\mathbf{r}(t) = \mathbf{G} + \mathbf{C} \cos(\Omega t) + \mathbf{S} \sin(\Omega t), \quad (4)$$

where vectors \mathbf{C} , \mathbf{S} contain respectively the modal cosine- and sine-components of forced vibration amplitudes and vector \mathbf{G} contains the modal components of the rotor-shaft static deflection due to the gravitational load. Then, by substituting (3) and (4) into (2) simplified for $\Omega = \text{const.}$ one obtains the following systems of linear algebraic equations:

$$\begin{aligned} \mathbf{K}(\Omega)\mathbf{G} &= \mathbf{Q}, \\ (\mathbf{K}(\Omega) - \Omega^2\mathbf{M}_0)\mathbf{C} + \Omega\mathbf{D}(\Omega)\mathbf{S} &= \mathbf{P}(\Omega^2), \\ (\mathbf{K}(\Omega) - \Omega^2\mathbf{M}_0)\mathbf{S} - \Omega\mathbf{D}(\Omega)\mathbf{C} &= \mathbf{R}(\Omega^2), \end{aligned} \quad (5)$$

These equations are very easy to solve with respect of the unknown components of vectors \mathbf{C} , \mathbf{S} and \mathbf{G} .

3. Numerical example of vibration analysis of the compressor rotor-shaft

The presented methodology of vibration analysis is applied here for the rotor-shaft of the considered eight-stage centrifugal compressor. The hybrid mechanical model of this rotor-shaft is shown in Fig. 2. With the aim of a sufficient geometrical and mechanical representation, the stepped-rotor shaft of this compressor

of the total length 2.8 m and total weight 485 kg has been modeled by means of $n = 23$ continuous macro-elements. More accurate modeling of such rotor-shaft system by means of a greater number of macro-elements does not introduce more detrimental computational efforts, but in the studied case it seems to be completely not necessary. All geometrical parameters of the successive real rotor-shaft segments together with their material constants as well as the average stiffness and damping coefficients of the oil-film in the bearings of this compressor have been taken from [12].

In the first step of dynamic analysis of the considered rotor-shaft an eigenvalue problem must be solved in order to obtain fundamental natural frequencies and corresponding eigenfunctions of bending and torsional vibrations. For the considered compressor rotor-shaft regarded here as dynamically isolated from the driving motor by means of the low-stiffness elastic coupling the torsional eigenvalue problem has been solved using the analogous hybrid (discrete-continuous) model described in [10, 11]. The obtained in this way lowest torsional natural frequency values 597.8 and 1212.4 Hz are far away above the fundamental first 10 bending natural frequencies determined using the Rayleigh beam theory and additionally confirmed by means of the Timoshenko theory.

Since for the reasons listed above the optimization procedure should be carried out not only for steady-state, nominal, out-of-resonance operating conditions, but for resonances excited during start-ups and run-downs of the compressor, the proper numerical simulation for such operation patterns has to be performed. In order to justify the proposed optimization methodology carried out for resonant operating conditions, in the first step a transient dynamic behavior of the considered rotor-shaft during compressor start-ups and run-downs must be demonstrated. For this purpose, an exemplary simulation of the system switch-on to switch-off operation cycle has been performed. Such exemplary cycle consists of the rotor-shaft start-up from its standstill to the nominal over-critical steady-state operation and of the rotor-shaft run-down, i.e. back to the standstill. It is assumed that the considered compressor is driven by an asynchronous motor by means of an elastic coupling, which dynamically isolates the compressor and motor rotor-shafts from each other. Thus, the carried out study can be focused on vibrations of the compressor rotor-shaft only. Since the first torsional natural frequency of this rotor-shaft is far above the fundamental 10 bending natural frequencies, during the investigated entire dynamic process flexural deformations of the shaft are predominant and the shaft torsional dynamic deformations seem to be negligible. According to the above, the considered rotor-shaft can be regarded as a torsionally rigid body rotating with a rotational speed gradually varying in time during start-

ups and run-downs. However, there are taken into consideration shaft bending vibrations induced by the system residual unbalance. For the assumed residual static unbalance uniformly distributed along each rotor-shaft cylindrical segment and for the concentrated static unbalances of each rigid body representing rotor-disks the external excitation is expressed by means of the following forcing terms:

$$\begin{aligned} p_i(x, t) &= \varepsilon_i \rho A_i \Omega^2(t) \sin(\Theta(t) + \psi_i) \quad \text{for } 0 < x < l_i, \quad i = 1, 2, \dots, n, \\ P_k(t) &= \varepsilon_k m_k \Omega^2(t) \sin(\Theta(t) + \psi_k) \quad \text{for } x = 0, \quad k = 1, 2, \dots, K, \end{aligned} \quad (6)$$

where $\varepsilon_i, \varepsilon_k$ denote the proper eccentricities caused by admissible manufacturing errors, ψ_i, ψ_k are the respective phase shift angles of the unbalance circumferential location with respect of the shaft rotation axis, K denotes the total number of rigid disks in the model and the remaining symbols have been already defined in Fig. 1 and in (2). For the assumed hybrid model of the investigated compressor rotor-shaft in the frequency range $0 \div 1000$ Hz 14 bending eigenmodes have been considered to solve equations (2) using the standard Newmark method with the time step 0.00002 s in order to achieve sufficiently high computational accuracy of the obtained results.

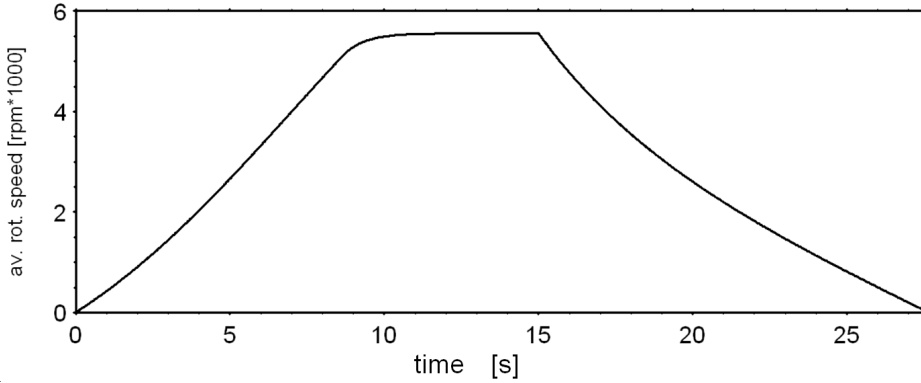


Figure 3: Time history of the rotor-shaft average rotational speed during start-up, nominal operation and run-down.

In Fig. 3 there is presented the time history of the average rotational speed $\Omega(t)$ of the rigid-body motion of the compressor rotor-shaft during start-up, steady-state nominal operation and run-down. This time history has been obtained by means of simulation of rigid-body rotational motion of the compressor entire drive system loaded by the electro-magnetic torque produced by the asynchronous motor according to [13] and the retarding torques caused by aero-dynamic forces in

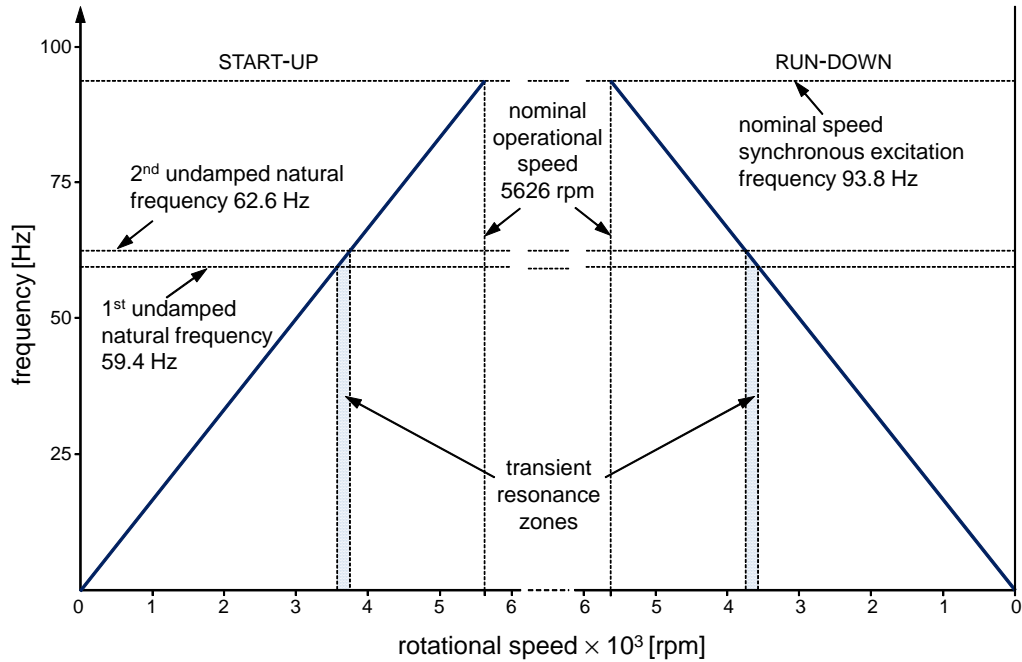


Figure 4: The Campbell diagram of the system operation.

the compressor stages. Temporary values of these retarding torques are assumed to be proportional to the square of the current shaft average rotational speed $\Omega^2(t)$. From this figure it follows that the start-up from the system rest till the nominal operation with the rotational speed 5626 rpm lasted ca. 10 s, the nominal operation lasted next 5 s and duration of the run-down amounted ca. 13 s. During the start-up and run-down the compressor rotor-shaft passed through the bending vibration resonance zones corresponding to the first two eigenmodes. Their natural frequency values determined for the undamped system are respectively equal to 59.4 and 62.6 Hz. These eigenmodes are induced to severe transient resonances by the synchronous excitation due to the unbalances when the rotor-shaft passes the average rotational speed range between 3500 and 3800 rpm, see Fig. 3 as well as Fig. 4 with appropriate Campbell diagram additionally demonstrating the considered compressor operation phases. The resonances result in a significant increase of bending vibration magnitude, which follows from Fig. 5 demonstrating the system lateral dynamic response corresponding to the variation of the shaft rotational speed during start-up, steady-state nominal operation and run-down shown

in Figs. 3 and 4. Here, the time history of the lateral displacement at the compressor shaft mid-span is depicted in Fig. 5a and the analogous time history of the transverse force in bearing #2 is shown in Fig. 5b.

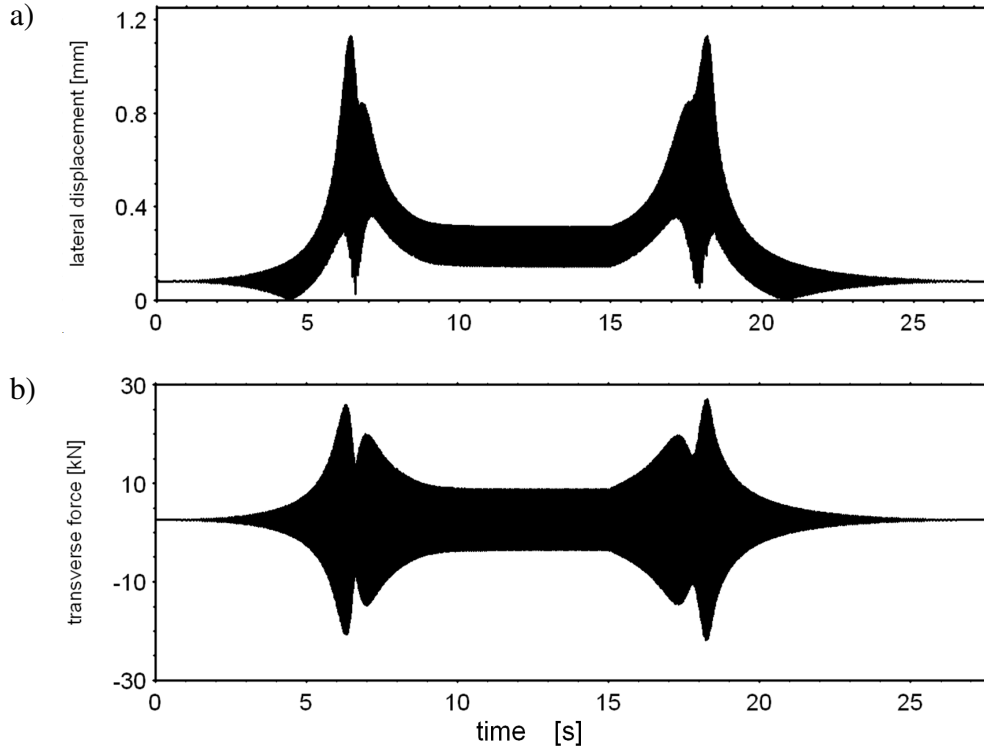


Figure 5: Time histories of the rotor-shaft response during start-up, nominal operation and run-down: (a) the lateral displacement of the shaft mid-span, (b) the transverse force in bearing #2.

As it follows from Figs. 5a and 5b, the passages through these resonances result in very significant increase of dynamic loading of the compressor rotor-shaft in comparison with the steady-state response for the nominal operating conditions at the rotational speed 5626 rpm. Each passage through the resonances causes ca. 3.6 times greater shaft lateral displacement amplitudes and ca. 3 times greater amplitudes of the bearing transverse forces. Such an increase of bending vibration magnitude must be associated with a probability of rubbing and with an analogous increase of the rotor-shaft material stresses, which can cause dangerous material fatigue upon a given number of routine successive switch-on switch-off cycles. This obvious fact substantiates a necessity of performing the rotor-shaft optimization procedure not for nominal operating conditions, but first of all, for the transient operation, i.e. for the resonant states.

According to the above, instead of the nominal, steady-state operation at 5626 rpm, which corresponds to synchronous excitation frequency 93.8 Hz, the optimization process is going to be performed for resonant working conditions. It is to remark that the carried out optimization procedure reduces to successive modifications of rotor-shaft diameters as well as to changes of the journal bearing stiffness and damping coefficients. Such parameter variations result in slight changes of the system natural frequencies. Here, the first two eigenfrequency values fluctuate within 54 – 67 Hz. Thus, in the case of each simulation the respective constant rotational speeds of the rotor-shaft have to correspond to these natural frequency values, at which maximum dynamic response is observed.

In the robust optimization example presented below the vibration response of the rotor shaft system has to be evaluated for thousands of realizations of the rotor-shaft parameters: unbalance amplitudes and their phase shift angles, bearing stiffness etc. For each set of parameters the analysis is carried out for resonant conditions with constant values of the shaft rotational speeds in the range 3240 – 4020 rpm, corresponding in every case to synchronous external excitation of the abovementioned fundamental bending eigenvibration modes. Here, for $\Omega = \text{const}$ in order to determine system steady-state dynamic responses, direct integration of (2) has been substituted by introducing the analytical solution, which leads to the straightforward and very effective to solve sets of algebraic equations (5). Similarly, as in the case of transient bending vibrations excited during start-up and run-down of the compressor, in order to obtain sufficiently high computational accuracy for steady-state lateral responses the above mentioned frequency range $0 \div 1000$ Hz containing 14 bending eigenmodes is taken into consideration for solving equations (5) in the framework of simulation based robust design optimization.

4. Formulation of the robust design optimization problem

Robust design is an engineering methodology for optimal design of products and structures that are less sensitive to system variations. It has been recognized as an effective design method to improve the product quality.

For structural design optimization problems, the structural performance defined by design objectives or constraints may be subjected to large scatter at different stages of the service life-cycle. Such scatters often not only significantly worsen the structural quality and cause deviations from the desired performance, but may also add to the life-cycle costs, including inspection, repair and other maintenance costs. From an engineering perspective, well-designed structures

minimize these costs by performing consistently in presence of uncontrollable variations of structural parameters. This raises the need of robust design where the goal is to find a design for which the structural performance is less sensitive to the variation of parameters without eliminating the cause of parameter variations. The idea of robustness is illustrated in Fig. 6 for a hypothetical one-dimensional design. Assuming constant variance of the design variable μ_X , being the expectation of a random variable X , the variance of the response is much smaller if $\mu_X = \mu_{X(2)}$, even though the mean response is smaller for $\mu_X = \mu_{X(1)}$. There are, however, cases where it is much more desirable to obtain low performance variability even at a price of worse mean performance than to have a design characterized by high performance, which is very sensitive to unavoidable parameter uncertainties.

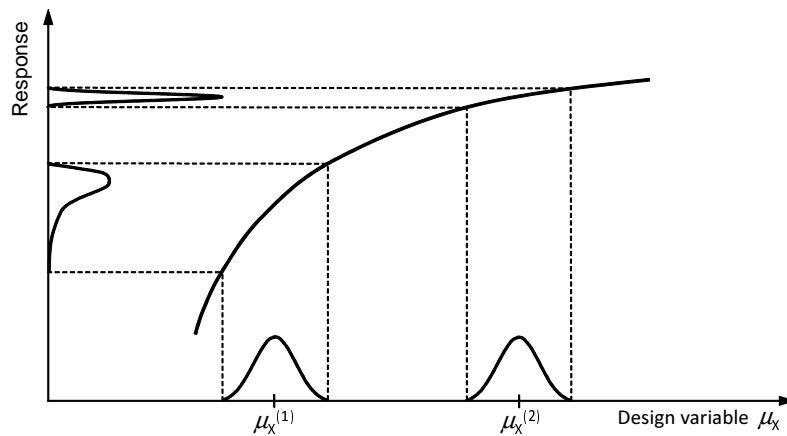


Figure 6: Concept of a robust design.

Therefore, the task to be performed in robust design optimization is to reduce the variability of the structural performance while improving its mean level. Basically, the variability of the structural performance can be roughly described by its standard deviation. However, other scatter measures are also being employed.

Mathematically a general formulation of the robust optimization problem can

be given as follows, cf. [8]:

$$\text{find: } \mathbf{d}, \boldsymbol{\mu}_{\mathbf{X}}, \quad (7)$$

$$\text{minimizing: } \tilde{f} = \frac{1-\alpha}{\hat{\mu}} \mathbb{E}[f(\mathbf{d}, \mathbf{X}, \mathbf{P})] + \frac{\alpha}{\hat{\sigma}} \sigma[f(\mathbf{d}, \mathbf{X}, \mathbf{P})], \quad (8)$$

$$\text{subject to: } \mathbb{E}[g_i(\mathbf{d}, \mathbf{X}, \mathbf{P})] - \beta_i \sigma[g_i(\mathbf{d}, \mathbf{X}, \mathbf{P})] \geq 0, \quad i = 1, \dots, k_g, \quad (9)$$

$$\sigma[c_l(\mathbf{d}, \mathbf{X}, \mathbf{P})] \leq {}^u\sigma_l, \quad l = 1, \dots, k_c, \quad (10)$$

$${}^l d_j \leq d_j \leq {}^u d_j, \quad j = 1, \dots, n_d, \quad (11)$$

$${}^l \mu_{X_r} \leq \mu_{X_r} \leq {}^u \mu_{X_r}, \quad r = 1, \dots, n_X, \quad (12)$$

where $\mathbf{d} \in \mathbb{R}^{n_d}$ is the vector of deterministic design variables, $\mathbf{X} \in \mathbb{R}^{n_x}$ is the vector of random design variables, $\mathbf{P} \in \mathbb{R}^{n_p}$ is the vector of random parameters and $\boldsymbol{\mu}_{\mathbf{X}}$ is the vector of mean values of \mathbf{X} variables that change during optimization. The functions f and g_i , $i = 1, \dots, k_g$, are the objective function and the constraint functions, respectively, $\mathbb{E}[\cdot]$ and $\sigma[\cdot]$ are the expectation and the standard deviation operators and c_l , $l = 1, \dots, k_c$, represent constraints on standard deviations of the selected responses. The parameter $\beta_i \geq 0$ is a prescribed feasibility index for the i -th constraint and ${}^u\sigma_l$ denotes the upper limit for the standard deviation of structural performance. The inequalities (11) and (12) form the side constraints on design variables. The factors $\hat{\mu}$ and $\hat{\sigma}$ in (8) are used for normalization and the weight factor $\alpha \in [0, 1]$ in function \tilde{f} is to investigate the trade-offs between the individual objectives. By setting $\alpha = 0$ the problem (7)-(12) can be converted to pure mean value minimization problem and for $\alpha = 1$ to pure minimization of the objective standard deviation.

The solution method employed for the rotor-shaft robust design optimization presented below consists of the two major elements: an efficient sampling technique for scatter analysis and an approximation method to create analytical meta-models of the objective and constraint functions.

In order to assess statistical moments necessary to compute values of functions (8)-(10) the so-called Latin hypercube (LH) random simulations are used. This descriptive sampling technique proved to be very efficient and superior to classical Monte Carlo sampling, see e.g. [14, 15]. While improving computational performance, LH sampling preserves the main advantage of random simulation techniques, i.e. the insensitivity to the shape of response functions.

Since the objective function \tilde{f} and the constraint functions (8) and (9) are implicit functions of the design variables it was decided to approximate them using the kriging technique, see [16]. The so-called MLE kriging (maximum likelihood

estimation) provides excellent fitting to the experimental points, but by its very nature is an interpolating rather than approximating method. This, however, can be considered as a drawback of this approach since functions (8)-(10) contain an unknown noise component due to the limited accuracy of the method of assessing the statistical moments. To overcome the problem of overfitting the kriging function to potentially noisy data, the approximative version of kriging, described in [17], has been used.

The main steps of the proposed solution strategy are as follows:

1. Create the trust region as a n -dimensional hypercube specified by the side constraints (11) and (12), where $n = n_d + n_x$.
2. Generate experimental points inside the trust region using the optimal Latin hypercube (OLH) plan of experiments, see [15]. The OLH plan provides an uniform sample distribution over the region.
3. For each generated point in the design space perform LH sampling to assess the values of $\mathbb{E}[f]$, $\sigma[f]$, $\mathbb{E}[g_i]$, $\sigma[g_i]$, $i = 1, \dots, k_g$, and $\sigma[c_l]$, $l = 1, \dots, k_c$. Store the computed objective and constraint values as well as the corresponding experimental points in the database.
4. Using all the data points that "fall" inside the current trust region build the kriging approximations of functions (8)-(10).
5. Find the current iteration of the optimal point \mathbf{d}^* , $\boldsymbol{\mu}_{\mathbf{x}}^*$ by solving the approximated optimization problem using a proper deterministic optimization algorithm.
6. Validate the obtained solution by performing additional LH sampling.
7. If the kriging approximation at the optimal point is satisfactory and the convergence criterion is satisfied then stop. If not, reduce the size of the trust region and return to step 2.

5. Example: robust design optimization of the compressor rotor-shaft

Consider a typical single-span compressor rotor-shaft system shown in Fig. 2. The optimization goal is to find such a shape of the rotor-shaft to reduce the probability that the lateral vibration amplitude excited by an unfavorable realization of random residual unbalances exceeds the admissible value, which in consequence may lead to rubbing effect.

The shape of the rotor-shaft is controlled by the diameters of 13 segments located between bearings, see Fig. 7. They are treated as deterministic design variables d_1, \dots, d_{13} . The nominal values of the diameters (in millimeters) are

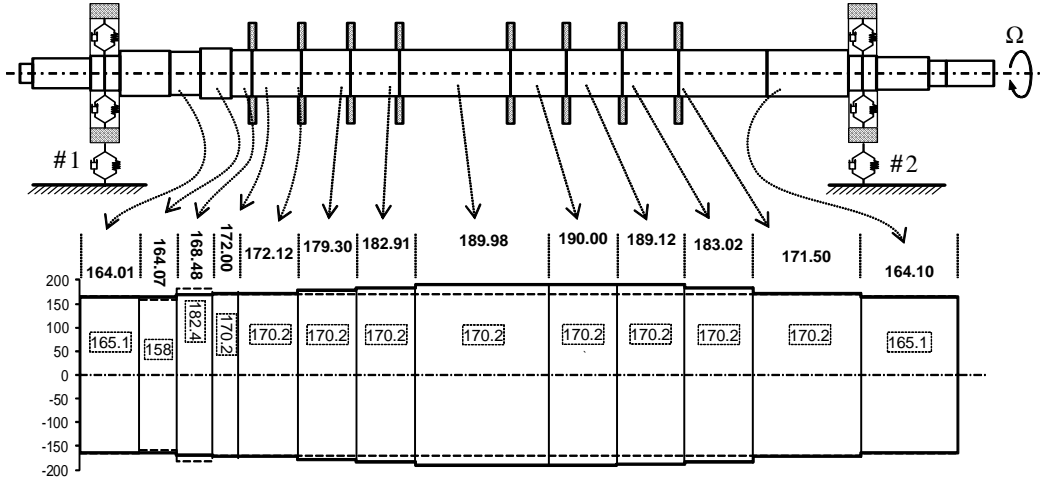


Figure 7: Nominal (dashed line) and the optimal (solid line) shapes of the rotor-shaft. The optimal values of the diameters are given above the corresponding segments and the nominal values are in the dashed boxes.

given in Fig. 7 inside the dashed line boxes. In absence of the random design variables $\mu_{\mathbf{X}}$, which are the expectations of selected random variables \mathbf{X} , the uncertain properties of the rotor-shaft system are modeled by 55 random parameters (\mathbf{P} type random variables). The stiffness as well as damping coefficients of the two journal bearings are represented by 16 normally distributed variables with the coefficients of variation equal to 10% for stiffness and 15% for damping coefficients. It was assumed that the distribution of residual unbalances (ε_i in Eq. (6)) can be modeled by a weighted function of 4 principal eigenmodes with the most probable contribution from the first eigenmode (with probability 0.8) and the probabilities of contributions from subsequent modes equal to 0.1, 0.08 and 0.02, respectively. The random magnitude of the unbalances is obtained by setting the maximal value of such constructed distribution function to be equal to a realization of log-normal random variable with expectation 0.15 mm and the standard deviation 0.02 mm. The remaining random parameters are 22 uniformly distributed phase shift angles (ψ_i in Eq. (6)) in the range $0 \div 2\pi$, 8 uniformly distributed rotor disk unbalances (ε_k in Eq. (6)) in the range $0 \div 1\text{mm}$ and finally 8 uniformly distributed rotor disk phase shift angles (ψ_k in Eq. (6)) in the range $0 \div 2\pi$.

The objective function f is taken to be the maximal vibration amplitude, which for most of the realizations of the vector of design variables \mathbf{d} and the vector

of random parameters \mathbf{P} occurs in the mid-span of the rotor-shaft. Three constraint functions are considered. The first one is imposed on the relative rotor-shaft to bushing displacement at the bearings. It takes the form $g_1(\mathbf{d}, \mathbf{P}) = q_b^a - q_b^{\max}(\mathbf{d}, \mathbf{P})$ where q_b^{\max} is the maximal relative displacement at bearings and q_b^a is the admissible one, set equal to 0.1mm. The second constraint, meant to prevent rubbing, has the similar form: $g_2(\mathbf{d}, \mathbf{P}) = q_r^a - q_r^{\max}(\mathbf{d}, \mathbf{P})$ but here q_r^{\max} is the maximal rotor-shaft displacement at its mid-span, where the rubbing effects are the most probable, and the admissible value $q_r^a = 0.7\text{mm}$. The third constraint is imposed on the structural volume. In the preliminary study it was found that it was not possible to fulfill the above mentioned constraints in the form given by Eq. 9 in the formulation of the robust design optimization problem. Therefore, it was decided to allow for up to 10% increase of the initial nominal volume, which leads to deterministic constraint function $g_3(\mathbf{d}) = 1.1V_{\text{nom}} - V(\mathbf{d})$, where V_{nom} is the nominal volume and $V(\mathbf{d})$ is the current volume. Finally, the rotor-shaft robust design optimization problem can be written as:

$$\text{find: } \mathbf{d} = \{d_1, \dots, d_{13}\}, \quad (13)$$

$$\text{minimizing: } \tilde{f} = \mathbb{E}[f(\mathbf{d}, \mathbf{P})]/\hat{\mu} + \sigma[f(\mathbf{d}, \mathbf{P})]/\hat{\sigma}, \quad (14)$$

$$\text{subject to: } \mathbb{E}[g_i(\mathbf{d}, \mathbf{P})] - 3.0\sigma[g_i(\mathbf{d}, \mathbf{P})] \geq 0, \quad i = 1, 2, \quad (15)$$

$$g_3(\mathbf{d}) \geq 0, \quad (16)$$

$$164\text{mm} \leq d_j \leq 190\text{mm}, \quad j = 1, \dots, 13. \quad (17)$$

Comparing with the general formulation (7)-(12) one can observe that none of the components of the composite objective function (14) is favored, which is equivalent to $\alpha = 0.5$, and that the "safety margins" in the constraint function definitions (15) are taken as $3.0\sigma[g_i(\mathbf{d}, \mathbf{P})]$, i.e. $\beta_i = 3.0, i = 1, 2$. The side constraints (17) have been selected basing on realistic practical engineering dimension limits existing for the investigated rotor-machine.

Due to the excellent computational performance of the employed numerical model and thanks to running the robust optimization task on 32 processor parallel machine it was possible to assume OLH-based designs of $10n = 130$ experimental points to create kriging response surfaces of the objective (14) and the constraints (15). To perform the scatter analysis, the samples of 2000 LH generated realization of random parameters were used. Using the available hardware it took about 12 hours to perform 1 iteration of the algorithm described in the previous section.

The optimal solution was found after 4 iterations. The optimal shape of the rotor-shaft and the values of segment diameters are shown in Fig. 7. By analyzing values of $\mathbb{E}[f]$ and $\sigma[f]$ estimated using LH sampling it was noticed that the two

quantities are positively correlated (not conflicting) and that the designs characterized by low mean value of the maximal vibration amplitude usually also produce low maximal amplitude scatter, see Fig. 8.

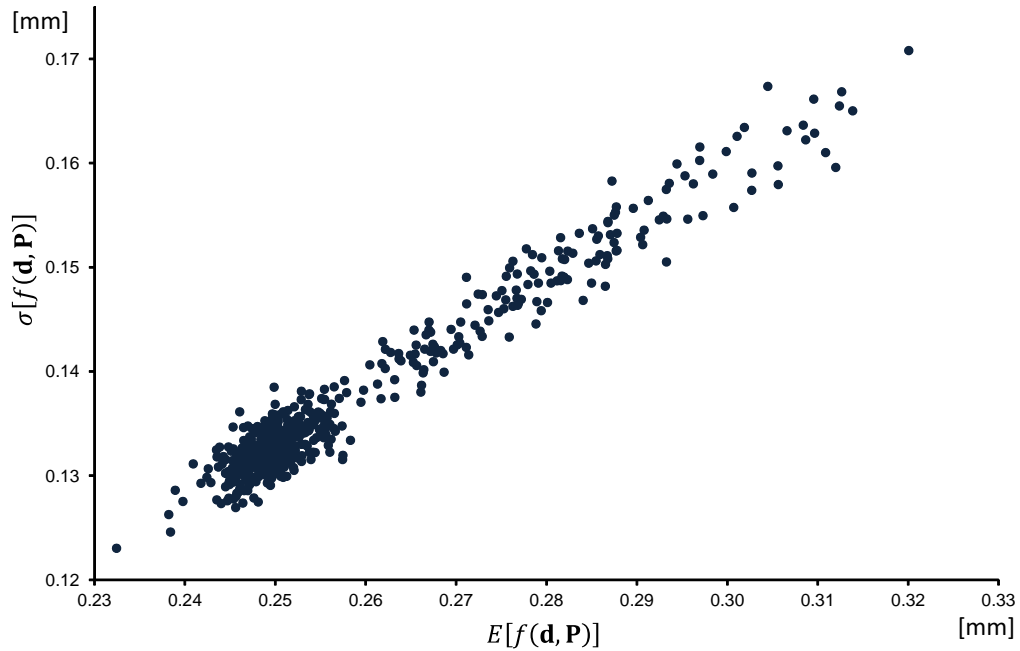


Figure 8: The objective function statistics obtained for various realizations of design variables.

It is interesting to compare the empirical probability density functions (PDFs) of the selected rotor shaft responses obtained for the nominal and for the optimal rotor-shaft designs. By looking at the PDFs shown in Fig. 9 it is clearly seen that the mean value of the maximal rotor-shaft displacement amplitude as well as its standard deviation decrease at the optimal solution. It is also extremely unlikely that a realization of the random rotor-shaft unbalances will lead to lateral displacements that are greater than the admissible 0.7mm. Therefore, the risk of rubbing is practically eliminated.

Contrary to the constraint imposed on the maximal mid-span displacement the constraint limiting the maximal relative rotor-shaft to bushing displacement at the bearings is not active at the optimal point. It turned out that the 3 sigma safety margin requirement has been already satisfied by the nominal project.

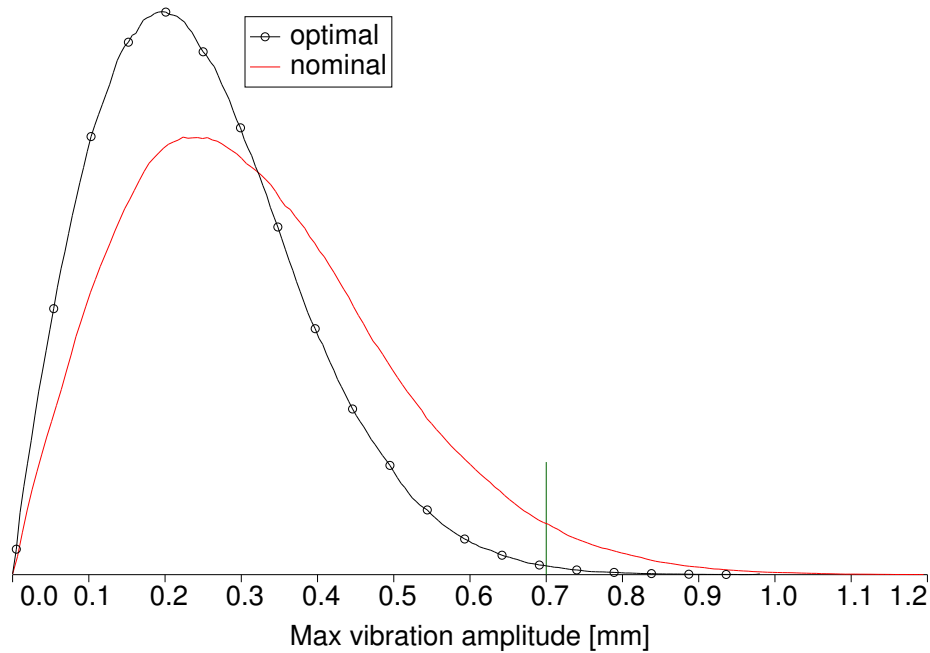


Figure 9: Empirical PDFs of the maximal rotor-shaft displacement amplitude.

6. Conclusions

The robust design optimization approach allows to account in the optimization process for the random nature of residual unbalances of the rotor-shaft as well as the randomness of journal bearing parameters. The proposed optimization algorithm has been applied for the optimization of the typical single-span rotor-shaft of the 8-stage centrifugal compressor. The obtained optimal rotor-shaft shape significantly reduces the risk of rubbing when the rotor-shaft system passes through the resonance excitation during start-ups and run-downs of the compressor.

The presented study is theoretical with the goal to create a solid basis for further experimental research aimed at verifying the obtained results and to introduce the methodology based on robust design optimization into engineering practice.

References

- [1] S. Bogomolov, V. Khavin, Composite algorithm for dynamic optimization of turbine rotors, *Strength of Materials* 8(5) (1976) 555–560.

- [2] P. Heam, Beasy used for optimization of rotor stress, in: C. A. Brebbia, J. J. Connors (Eds.), Proc. 11th Int. Conference on Boundary Element Method, Advances in Boundary Elements, Vol. 3, Stress Analysis, 1989, pp. 436–450.
- [3] D. Bondoux, D. Doizelet, Dynamic optimization of a rotor-bearing set, in: Proc. 12th Biennial ASME Conference on Mechanical Vibration and Noise, 18-1, ASME, Rotating Machinery Dynamics, Montreal, Canada, Vol. 18-1, 1989, pp. 11–16.
- [4] D. Doizelet, D. Bondoux, Application of optimization techniques for hypercritical rotors, in: Proc. 3rd Int. Rotordynamics Conference, IFToMM, Editions du CNRS, Lyon, France, 1990, pp. 57–62.
- [5] W. Diewald, R. Nordmann, Parameter optimization for the dynamics of rotating machinery, in: Proc. 3rd Int. Rotordynamics Conference, IFToMM, Editions du CNRS, Lyon, France, The University of Michigan, Ann Arbor, 1990, pp. 51–56.
- [6] H. Kanki, K. M., K. Ono, Rotor balancing method using LMI optimization, Trans. of the Japan Society of Mech. Engineers C 65(634) (1999) 2218–2225.
- [7] Y. Tsompanakis, N. Lagaros, M. Papadrakakis (Eds.), Structural Design Optimization Considering Uncertainties, Structures and Infrastructures Series, Taylor and Francis, 2007.
- [8] Z. Kang, Robust design optimization of structures under uncertainty, Ph.D. thesis, Institut für Statik und Dynamik der Luft- und Raumfahrtkonstruktionen Universität Stuttgart (2005).
- [9] H.-G. Beyer, B. Sendhoff, Robust optimization - A comprehensive survey, Computer Methods in Applied Mechanics and Engineering 196 (2007) 3190–3218.
- [10] T. Szolc, On the discrete-continuous modeling of rotor systems for the analysis of coupled lateral-torsional vibrations, Int. Journal of Rotating Machinery 6 (2) (2000) 135–149.
- [11] T. Szolc, P. Tuzowski, R. Stocki, J. Knabel, Damage identification in vibrating rotor-shaft systems by efficient sampling approach, Mechanical Systems and Signal Processing 23 (2009) 1615–1633.

- [12] J. Vázquez, L. Barrett, Modeling of tilting-pad journal bearings with transfer functions, in: "Proc. 7th Int. Symposium on Transport Phenomena and Dynamics of Rotating Machinery, ISROMAC-7, Honolulu, Hawaii, February (1998)", Vol. A, 1998, pp. 472–481.
- [13] A. Laschet, Simulation von antriebssystemen, Structural Engineering and Mechanics, Springer-Verlag, Berlin, Heidelberg, London, New-York, Paris, Tokyo.
- [14] R. Stocki, P. Tazowski, M. Kleiber, Efficient sampling techniques for stochastic simulation of structural systems, Computer Assisted Mechanics and Engineering Sciences 14 (2007) 127–140.
- [15] M. Liefvendahl, R. Stocki, A study on algorithms for optimization of Latin hypercubes, Journal of Statistical Planning and Inference 136 (2006) 3231–3247.
- [16] D. Jones, M. Schonlau, W. Welch, Efficient global optimization of expensive black-box functions, Journal of Global Optimization 13 (1998) 455–492.
- [17] M. Sasena, M. Parkinson, M. Reed, P. Papalambros, P. Goovaerts, Improving an ergonomic testing procedure via approximation-based adaptive experimental design, ASME Journal of Mechanical Design 127 (2005) 1006–1013.